Experiments and simulations of low Re sphere wakes with and without stratification

X. Xiang, K.K. Chen, T.J. Madison, P. Sellappan and G.R. Spedding

Department of Aerospace and Mechanical Engineering,
University of Southern California, Los Angeles
xinjianx@usc.edu, geoff@usc.edu

Abstract

Near wakes behind a sphere in both homogeneous and linearly stratified background were studied numerically and experimentally at Reynolds number Re ≤ 1000, Froude number Fr ≥ 0.5. In a homogeneous fluid, the structural transitions with increasing Re are consistent with previous studies. The stratified results from simulations and experiments are in good agreement. Stratified wakes undergo similar transitions with decreasing Fr for Re in current range, except that similar transitions occur at larger Re as Fr decreases, thus making the wake structure at high Re, low Fr similar to that at low Re, high Fr.

1   Introduction

Bluff body wakes in both stratified and unstratified background have been studied extensively due to their geophysical and naval applications. Both simulations and experiments have shown the dependence of near-wake structures on initial Re and Fr, and a global map of the wake structure behind a towed sphere has been provided by Lin et al. (1992) and Chomaz et al. (1993).

Nevertheless, in the regime where the near wake is fully turbulent, despite the initial degree of turbulent kinetic energy, the wake eventually evolves into a state dominated by low Fr dynamics with persistent patterns (Spedding, 1997), and the memory of the wake-generating body shape is lost (Meunier and Spedding, 2004). The same observation also justifies the temporal simulations of the far wake with a patch of turbulence superimposed on a Gaussian-shape mean profile (Gourlay et al., 2001; Dommermuth et al., 2002; Diamessis et al., 2011) with no generating body. The driving mechanisms, and structural transition from the near wake that does depend on initial conditions, have been debated continuously without the benefit of detailed quantitative near-wake data, whose secondary purpose would also be to properly initialize temporal simulations.

In the low Re regime, where the flow is not turbulent, the stratification effect is obvious since the near-wake structure undergoes distinct transitions between varying Fr and Re. Early experiments visualized these different wake structures with shadowgraph techniques, dye tracers and particle streaks (e.g. Lin et al. (1992); Chomaz et al. (1993)). Meanwhile, corresponding direct numerical simulations (DNS) were limited to very low Re (e.g. Hanazaki (1988)). The full-field measurement of the near wake for a wide range of Re and Fr was shown possible recently in both experiments (Xiang et al., 2015) and DNS (Orr et al., 2015).

In a similar spirit as Lin et al. (1992) and Chomaz et al. (1993), we present here a comparative study of PIV experiments and DNS at various Reynolds number Re $= 2UR/\nu = \{200, 300, 500, 1000\}$, and Froude number Fr $= U/(NR) = \{0.5, 1, 2, 4, 8, 16, \infty\}$, where U is the towing velocity in experiments or incoming flow speed in simulations, R is the

radius of the sphere, and N is the buoyancy frequency. Re and Fr are selected so that the near wake traverses through a number of characteristic flow regimes. The full-field measurement allows for accurate and detailed description of the wake structure and evolution. The similarity between wakes of different Re and Fr can now be evaluated quantitatively, the conclusion of which may also be implied for higher Re flows.

2 Numerical methods

The unstratified wake problem is represented by the incompressible continuity equation and Navier-Stokes equation without gravitational force. For stratified cases, given the initial stratification in the z direction, the density and pressure fields are decomposed into mean and fluctuating parts as $\rho(\mathbf{x}, t) = \overline{\rho}(z) + \rho'(\mathbf{x}, t)$ and $p(\mathbf{x}, t) = \overline{p}(z) + p'(\mathbf{x}, t)$. After applying the Boussinesq approximation and hydrostatic balance, the equations to be solved can be simplified as

$$\nabla \cdot \mathbf{u} = 0, \tag{1}$$

$$\frac{\partial \mathbf{u}}{\partial t} + \mathbf{u} \cdot \nabla \mathbf{u} = -\nabla p' + \nu \cdot \nabla^2 \mathbf{u} + \rho' \mathbf{g}, \tag{2}$$

$$\frac{\partial \rho'}{\partial t} + \mathbf{u} \cdot \nabla \rho' = w \cdot \frac{d\overline{\rho}}{dz} + \alpha \cdot \nabla^2 \rho', \tag{3}$$

where $\mathbf{u}$ is the velocity field, $\mathbf{g}$ is the gravitational acceleration constant in z direction, α is the thermal diffusivity, and ν is the kinematic viscosity. In current simulations, the inlet flow velocity and sphere diameter are fixed, so Re and Fr are modified by changing ν and $d\overline{\rho}/dz$.

The equations are solved using programs based on OpenFOAM suite, a finite volume method solver. The temporal and spatial derivatives are discretized using second order accuracy schemes, and the whole algorithm is also second order accurate. The computational domain is $32R \times 32R \times 120R$, but we only take the results in the near wake up to $30R$ downstream. A coarse mesh with about 3 million cells is used for Re $= \{200, 300, 500\}$, and a fine mesh with about 17 million cells is used for Re $= 1000$. To reduce internal wave reflection from the boundaries, zero gradient boundary condition is adopted for side boundaries. Initially, the sphere is oscillated back and forth once in all axes to break flow symmetry (Lee, 2000).

3 Experimental methods

Experiments were conducted by horizontally towing a sphere in a 1m $\times$ 1m $\times$ 2.5m tank. The sphere was suspended from a translation stage using the same three-wire method as Chomaz et al. (1993), except that a 3D printed shell was ballasted with a steel bearing ball to stabilize the setup. The average kinematic viscosity in the stratified wake region was $\nu \approx 1.005 \times 10^{-6}$ m^2/s. The buoyancy frequency $N = [(-g/\rho_0) \cdot (d\rho/dz)]^{0.5}$, where ρ_0 is the reference density, was maintained the same for cases of the same Re, i.e. $N = \{0.27, 0.2, 0.33, 0.33\}$ for cases of Re $= \{200, 300, 500, 1000\}$, respectively. Spheres of radius $R = \{5.5, 3.9, 2.7, 1.9, 1.4, 0.99, 0.72\}$ cm were towed at corresponding speeds to achieve the designed Re and Fr combinations.

Two side-by-side cameras along the stream-wise direction, each with a field of view (FOV) of size 30 cm $\times$ 35 cm, were set to record images. Spheres were towed for 70 cm before

entering the FOV to avoid startup effects. Two velocity components $\{u, w\}$ in the vertical $x - z$ center-plane were estimated using PIV with sampling rates of $\{5, 10, 20\}$ Hz depending on the towing velocity. A refractive index matching technique as detailed in Xiang et al. (2015) was employed to reduce optical distortions due to early-time sharp density gradients.

4 Results and Analysis

4.1 Unstratified wakes results

Early experiments and simulations have investigated the unstratified wakes behind a sphere at Re $\leq$ 1000 (e.g. Achenbach (1974); Tomboulides and Orszag (2000)). Here, the unstratified wakes results can be compared with literature results and then used for comparison with stratified equivalents.
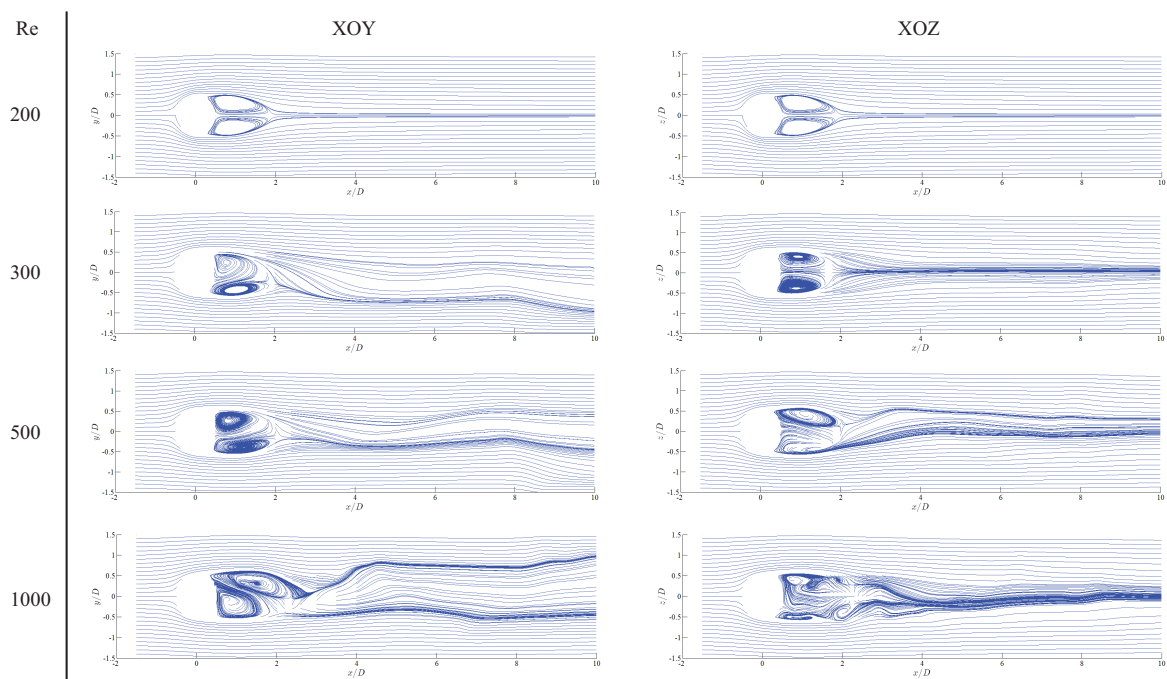

Figure 1: Simulation results of streamlines constructed from in-plane velocities for flow past a sphere at varying Re.

The streamlines are shown in figure 1 for unstratified flow in simulations. Note that the lines are not the true 3D streamlines due to the presence of out-of-plane velocity, but they provide clear ideas of the wake structure. The wake at Re = 200 is axisymmetric, and has a recirculation region of length $1.4D$, where $D = 2R$ is the diameter of the sphere. At Re = 300, with weak initial perturbation, the wake cannot maintain axisymmery, but oscillates at $St = fD/U = 0.133$ in one plane, where f is the oscillating frequency, while keeping planar symmetry in the other plane. The plane in which the wake oscillates depends on the initial perturbation, but in our experiments, it was observed to be affected also by intermediate perturbations. The spiral mode forms at Re = 500, and in a convective time window of 250, a dual-frequency oscillation at $St = 0.168$ and $St = 0.044$ is recorded. The wake becomes more irregular at Re = 1000. A lower frequency is found at $St = 0.191$,

and another higher frequency around 0.33, but much less dominating than the lower-frequency peak. All these structural transitions and frequency measurements agree well with existing experiments (Achenbach, 1974; Kim and Durbin, 1988) and simulations (Tomboulides and Orszag, 2000; Lee, 2000).
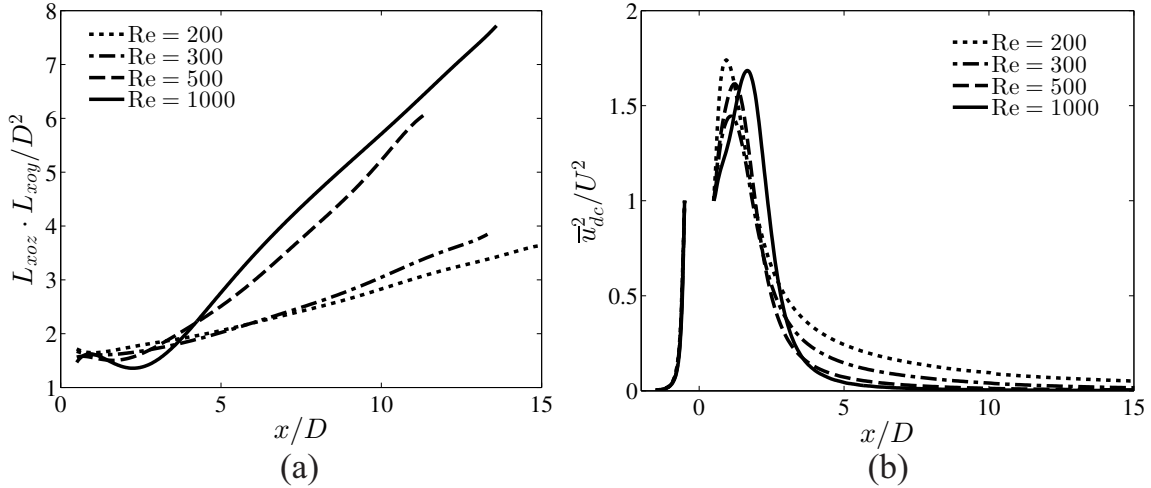

Figure 2: Simulation results of unstratified wakes at varying Re: (a) dimensions and (b) centerline defect velocity.

Increasing Re not only changes the structure of the wake, but also affects the kinetic energy distribution. Following other studies, we define defect velocity $\overline{u}_d = U - \overline{u}$, where $\overline{u}$ is the mean local stream-wise velocity, and define $\overline{u}_{dc}$ as the centerline defect velocity along x axis. Then the wake edge can be defined as the location where $\overline{u}_d = 0.15\overline{u}_{dc}$, and thereafter the wake height and width can be defined as the distance between the wake edges in XOZ and XOY planes, respectively, denoted as L_{xoz} and L_{xoy}. Since the defect velocity fields at these Re are gaussian-shape, we can very roughly indicate the area of the wake region by $L_{xoz} \cdot L_{xoy}/D^2$, and kinetic energy by $\overline{u}_{dc}^2/U$. Both results are shown in figure 2. The oscillation motion appears to help with the wake propagation by entraining more outer flow, and therefore making the energy more dispersed. For Re ≤ 1000, increasing Re makes the wake region larger at the same downstream distance, but also results in a faster decay in centerline defect velocity.

4.2 Stratified wakes results

For stratified cases, the drag coefficients computed from simulations, and lee wave wavelength measured in both experiments and simulations, agree well with previous studies (e.g. Lofquist and Purtell (1984); Hanazaki (1988); Chomaz et al. (1993); Orr et al. (2015)). The structural characteristics at varying Fr and Re shown in our simulations also agree well with those in our experiments. All these results will be reported later elsewhere.

Comparisons of wake height and centerline defect velocity between simulations and experiments are plotted in figure 3 for selected Re and Fr. Results from Camera 1 and Camera 2 are in good agreement, indicating that the startup effects should have dissipated. The oscillation in wake height signals the presence of lee waves, and affects the
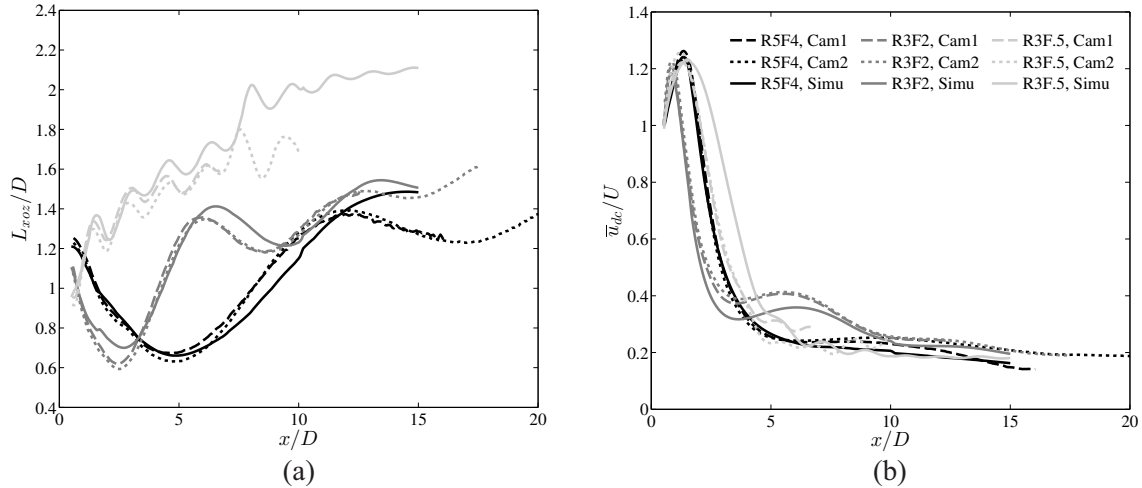
Figure 3: Comparison of experimental and numerical results: (a) wake height and (b) centerline defect velocity. Here R5F4 indicates $Re = 500, Fr = 4$, and similarly for R3F2 and R3F.5. Legends are the same for both plots. Results from Camera 1, Camera 2, and simulations are shown here.

centerline velocity by changing the flow area. This kind of "nozzle effect" is also observed for grid wakes (Xiang et al., 2015), and is more obvious for smaller Fr when $Fr \geq 1$, but opposite when $Fr < 1$ since the lee wave magnitude decreases. The simulation results also agree fairly well with the experiments, except that there is usually a small difference in the phase of lee wave. The difference beyond $x/D = 10$ is larger as the mesh becomes coarser for $x/D > 10$, so numerical dissipation also increases from here on. The difference is generally greater for very low Fr cases, likely as the mesh is not sufficiently fine to fully resolve the severe stratification.

The wake structures at different Re and Fr were described with experimental photos in Lin et al. (1992) and Chomaz et al. (1993). Here the simulation results of streamlines in XOY and XOZ planes are presented in figure 4 for selected Re and Fr. For $Re = 200$, decreasing Fr compresses the wake height, therefore breaking axisymmetry while maintaining planar symmetry in both planes. The lee wave pattern can be clearly observed at low Fr, and becomes saturated at $Fr = 1$. When Fr is further decreased below unity, the kinetic energy is not sufficient to move centerline fluid particles over the dome, so more of them go around the sphere. By $Fr = 0.5$, an oscillating tail of frequency $St \approx 0.2$ is observed in the XOY plane, while the wake in XOZ plan is still planar symmetric. Further decreasing Fr likely requires a much finer resolution for the severe stratification (Orr et al., 2015), therefore is not covered here. One would expect the wake to eventually resemble that behind a cylinder, where vortex shedding occurs (see Lin et al. (1992) and Chomaz et al. (1993)). When the wake is weakly stratified, the wake structure for $Re = 300$ is similar to that in the unstratified case. At $Fr = 4$, the wake of $Re = 300$ is nonoscillating but asymmetric in XOY plane, in contrast to the wake of $Re = 500$ where it is still oscillating. Planar symmetry is recovered at $Fr = 2$ for both Re, and further decreasing Fr makes the wakes go through same transitions as those in $Re = 200$. Similarly for $Re = 1000$, oscillations in the XOZ plane first disappear as Fr decreases, while the wake in XOY plane remains disorganized even at $Fr = 2$, and the wake is planar symmetric at $Fr = 1$.
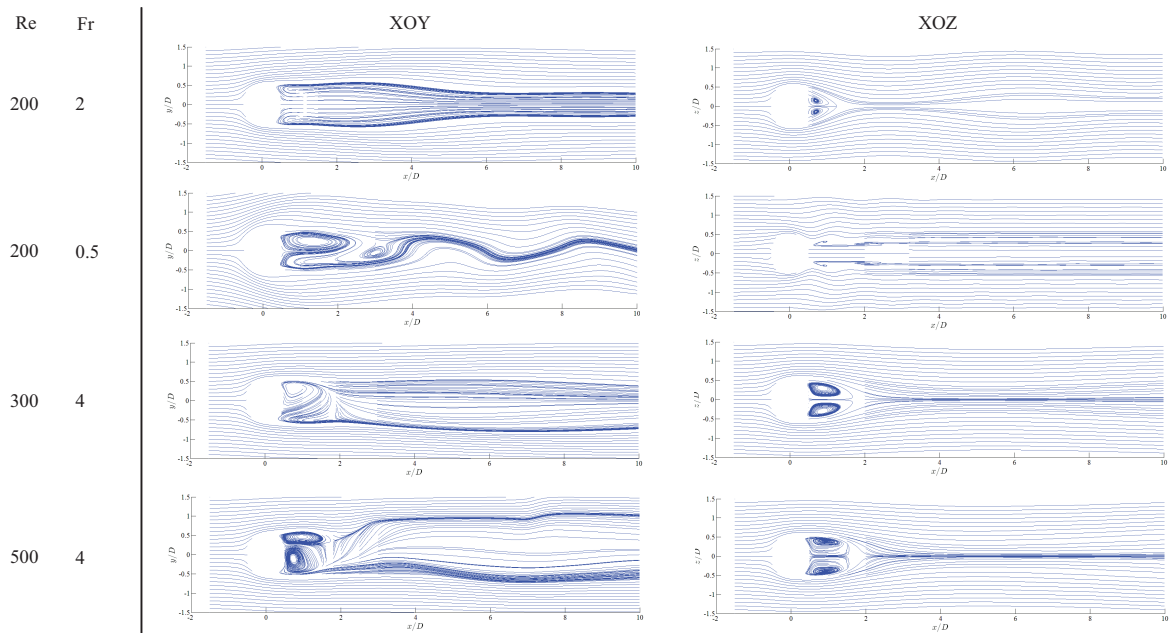
Figure 4: Simulation results of streamlines constructed from in-plane velocities for stratified flow past a sphere at selected Re and Fr.

5 Conclusions

A comparative study of experiments and DNS is conducted to quantify the wakes behind a sphere at various Re $\leq$ 1000 and Fr $\geq$ 0.5. Without stratification, the wake is more unsteady with increasing Re, and the structural transitions are consistent with previous studies. The oscillatory motions at larger Re increase lateral propagation, and disperse kinetic energy over a broader area. For stratified wakes, the simulations agree well with experiments. A "nozzle effect" can be observed due to lee waves, and is more obvious when Fr $\simeq$ 1. In the current range of Re, decreasing Fr works as a stabilizer when Fr $\geq$ 1, but a destabilizer when Fr $<$ 1: it first eliminates vertical oscillation, then horizontal oscillation, and then recovers planar symmetry; horizontal oscillation reoccurs when Fr $<$ 1. This transition procedure is similar for all current Re, starting from their unstratified wake structure, except that a similar transition occurs at a lower Fr for a higher Re. If the stabilizing effects of stratification persist at much higher Re when the flow is turbulent, similarities may exist between high Re, low Fr flows, and low Re, high Fr flows, which are easier to realize in lab experiments.

Acknowledgements

References

Achenbach, E. (1974). Vortex shedding from spheres. *J. Fluid Mech.*, 62:209.

Chomaz, J. M., Bonetton, P., and Hopfinger, E. J. (1993). The structure of the near wake of a sphere moving horizontally in a stratified fluid. *J. Fluid Mech.*, 254:1–21.

Diamessis, P. J., Spedding, G. R., and Domaradzki, J. A. (2011). Similarity scaling and vorticity structure in high-Reynolds-number stably stratified turbulent wakes. *J. Fluid Mech.*, 671:52–95.

Dommermuth, D. G., Rottman, J. W., Innis, G. E., and Novikov, E. A. (2002). Numerical simulation of the wake of a towed sphere in a weakly stratified fluid. *J. Fluid Mech.*, 473:83–101.

Gourlay, M. J., Arendt, S. C., Fritts, D. C., and Werne, J. (2001). Numerical modeling of initially turbulent wakes with net momentum. *Phys. Fluids*, 13:3783–3802.

Hanazaki, H. (1988). A numerical study of three-dimensional stratified flow past a sphere. *J. Fluid Mech.*, 192:393–419.

Kim, H. J. and Durbin, P. A. (1988). Observations of the frequencies in a sphere wake and of drag increase by acoustic excitation. *Phys. Fluids*, 31:3260–3265.

Lee, S. (2000). A numerical study of the unsteady wake behind a sphere in a uniform flow at moderate reynolds numbers. *Comput. Fluids*, 29(6):639–667.

Lin, Q., Lindberg, W. R., Boyer, D. L., and Fernando, H. J. S. (1992). Stratified flow past a sphere. *J. Fluid Mech.*, 240:315–354.

Lofquist, K. E. and Purtell, L. P. (1984). Drag on a sphere moving horizontally through a stratified liquid. *J. Fluid Mech.*, 148:271–284.

Meunier, P. and Spedding, G. R. (2004). A loss of memory in stratified momentum wakes. *Phys. Fluids*, 16:298–303.

Orr, T. S., Domaradzki, J. A., Spedding, G. R., and Constantinescu, G. S. (2015). Numerical simulations of the near wake of a sphere moving in a steady, horizontal motion through a linearly stratified fluid at Re = 1000. *Phys. Fluids*, 27(3):035113.

Spedding, G. R. (1997). The evolution of initially turbulent bluff-body wakes at high internal Froude number. *J. Fluid Mech.*, 337:283–301.

Tomboulides, A. G. and Orszag, S. A. (2000). Numerical investigation of transitional and weak turbulent flow past a sphere. *J. Fluid Mech.*, 416:45–73.

Xiang, X., Madison, T. J., Sellappan, P., and Spedding, G. R. (2015). The turbulent wake of a towed grid in a stratified fluid. *J. Fluid Mech.*, 775:149–177.